MET.O.14

METEOROLOGICAL OFFICE
BOUNDARY LAYER RESEARCH BRANCH
TURBULENCE & DIFFUSION NOTE

T.D.N. No. 53

An Observation of waves and turbulence in the Earth's Boundary Layer.

by

S.J.Caughey and C.J.Readings

July 1974

FH1

An Observation of waves and turbulence in the Earth's Boundary Layer

by

S. J. Caughey and C. J. Readings

1. Introduction:- The interpretation of atmospheric data obtained in stable conditions may well be complicated by the coexistence of turbulence and internal gravity waves. These two phenomena have quite different properties and it is important to distinguish between them if erroneous deductions are to be avoided. This problem was discussed extensively during the Colloquium on Spectra of Meteorological Variables which was held at Stockholm in June 1969 (see Stewart (1969) and Busch (1969)). Various ways of distinguishing between these two types of motion were proposed. One of these is based on the spectral characteristics of the temperature and velocity fields and has been used by Axford (1971) to evaluate some observations of gravity waves in the lower stratosphere. This paper describes an observation of waves and turbulence in the first two hundred metres of the Earth's boundary layer under stable stratification. The detailed analysis of the data illustrates the complexities introduced by advection and the proximity of the surface. These results were obtained during the night of 31st November/ 1 December, 1972 at Cardington (Beds.) as part of a radiation fog study.

2. Instrumentation:- Four Cardington turbulence probes were used to simultaneously measure the flow characteristics of the atmospheric boundary layer at heights of 8, 46, 93 and 183 metres. These instruments measured the instantaneous values of the wind flow to the horizontal (ϕ), the total wind speed (V) and the temperature (T) - see Readings and Butler (1972). The lowest two instruments were mounted on fixed supports whilst the others were attached to the flying cable of a tethered kite balloon (1300 cu. metres capacity). All the variables were sampled once a second and the values punched on paper tape. These were subsequently processed by an ICL 1900 computer.

In addition to the turbulence probe data, the mean temperatures (wet and dry) and the mean wind speed were recorded at various levels between 0.2 and 16 metres as well as the mean wind direction at 16 metres. The Cardington Balthum (Painter, 1970) was used to measure the profiles of wind, temperature and humidity up to 900 metres.

3. <u>The Data</u>:- The traces of the three basic quantities (T, ϕ and V) for the four probes during part of the night 30th November/1 December 1972 are reproduced in Fig. 1. Between about 0140 and 0224 GMT it is clear that all the traces exhibit "wave-like" characteristics. These are more clearly illustrated in Fig. 2 which shows 30 secs.average values plotted with expanded vertical scales. The wave is clearest at the highest level (i.e. 183 m) where the flow was smooth and essentially free of turbulence before and during the period of the wave.

At 183 m. the amplitude of the T and V oscillations are about 0.7°C and 2 ms^{-1} respectively; with the flow occasionally reaching 15-20 degrees inclination. A comparison of the T traces at this height and at 93 m shows the lower level lags the upper one by about one minute. From 0153 GMT onwards there are "bursts" of turbulent activity on all the 93 m traces. These seem to be associated with the crests in the ϕ trace. Similar "bursts" are visible at 46 metres after 0140 GMT but these appear to precede those at 93 metres (this will be discussed later). At the lowest level (8 m) the passage of the wave is most closely shown by the V -trace as the ϕ -trace exhibits significant levels of turbulence throughout this period. However even at this low level there is some indication of an increase in turbulent activity associated with the passage of the wave. At all levels the temperature shows significant trends during the period of the wave and this may indicate that the wave was associated with the slow moving cold front which was in the vicinity at this time.

The variations of the wind direction at 16 m., over the period of the wave are shown in Fig. 3 and it can be seen that the advent of the wave was associated with a change in the wind direction from 170°N to 300°N. Furthermore there are indications of "wave-like" oscillations between 0145 and 0220 GMT similar to those reported by Gossard et al (1970). Inset in Fig. 3 are the wind direction and speed traces at 46 m recorded by the Met. Office anemograph at Cardington. The wind direction trace reproduces the main features present at 16 m and the regularly spaced wind maxima are clearly resolved.

In Fig. 4 the dry bulb and dew point temperatures from the 2300/0020 GMT Balthum ascent are plotted as a function of height. These show a surface inversion extending upwards to about 200 m with the region close to the surface near saturation. This figure also includes a plot of the profile of the virtual potential temperature (Θ_V) and the corresponding values of the Brunt - Väisälä frequency (N):-

$$N = \sqrt{\frac{g}{\Theta_V} \frac{d\Theta_V}{dz}} \qquad (1)$$

for the various layers. The values show that at about 200 m gravity waves could not have a frequency higher than about 0.02 sec^{-1}, since if the wave frequency (ν) exceeds the local value of N the propagation vector in the vertical becomes imaginary and wave will be dissipated (see Gossard et al (1971)). Furthermore a wave with a frequency in the range 0.002 to .02 sec^{-1} could be trapped below 300 m since N decreases by an order of magnitude above this level. Although these values strictly describe conditions 1½-2 hours before the period of interest the changes (deduced from the next Balthum ascent 6 hours later) were small and do not significantly affect the figures.

4. Spectral Analysis:- Using the Fast-Fourier transform algorithm (see Rayment (1972)) a spectral analysis was carried out on the one second u, w and T values (w is the vertical wind component and u the horizontal one). For each probe the following quantities were derived

a. the cross-spectral amplitude $Sxy(n) = \sqrt{C_{xy}^2(n) + Q_{xy}^2(n)}$ where x and y represent the signals;

$C_{xy}(n)$ and $Q_{xy}(n)$ are the co- and quadrature spectra respectively at frequency n. $Sxy(n)$ is a measure of the average energy shared by the two signals at a particular frequency.

b. the phase angle $\Phi_{xy}(n) = \tan^{-1} \frac{Q_{xy}(n)}{C_{xy}(n)}$. This represents the phase difference between the common frequency components of the two signals.

c. The coherence $coh_{xy}(n) = \frac{S_{xy}(n)}{S_x(n) S_y(n)}$ where $S_x(n)$ and $S_y(n)$ are the two individual power spectra at frequency n. This gives a measure of the correlation between the two signals as a function of frequency. These quantities were calculated for all combinations of the variables u, w, T.

It is apparent from Fig. 1 that the intensity of turbulence increases as the level of observation approaches the ground. This was confirmed by integrating $S_w(n)$ over the frequency range $10^{-2} < n < 10^{-1}$ sec^{-1}. The results are reproduced in Table 1. This shows that the high frequency w - fluctuations increased by more than an order of magnitude between 183 and 46 metres. The wave characteristics will therefore be most clearly revealed by the results at 183 m.

When a wave is present the spectra/cross-spectra should exhibit peaks associated with high levels of coherence and stable phase angles. This is precisely what was obtained at 183 m (see Fig. 5). All the spectra have pronounced peaks in the frequency range $.002 < n < .003$ sec^{-1} (note that the ordinates are $n\, S(n)$ etc., but the position of these peaks is not significantly changed by altering the ordinate to $S(n)$ etc). This corresponds to a period lying between 5 and 8 minutes. The coherences at these frequencies are much closer to the ideal value of unity than those reported by Axford (1971) - see Table 2. This table also lists the phase angles between the various components and it can be seen that Axford's values are quite different from the present ones although both form a self consistent set (i.e. $\Phi_{wu}(n) + \Phi_{uT}(n) + \Phi_{Tw}(n) \approx 0$). In the present case of a stable temperature profile and reversed wind gradient the following values would have been expected

$$\Phi_{wT}(n) = 90^\circ$$
$$\Phi_{uT}(n) = 180^\circ$$
$$\Phi_{uw}(n) = 90^\circ$$

(these values are also applicable to Axford's case). It can be seen that though Axford's values are in fairly good agreement with the theoretical ones the present values are quite different. This anomaly will be considered further in the next section.

As the level of observation approached the ground,

(i) turbulence and advection became more significant

(ii) the spectral peaks were much less prominent

(iii) coherences decreased to .2-.6

(iv) the phase angles were poorly defined.

The slope of the spectra (i.e. $S_x(n) \propto n^{-5}$) provides a good indication that the peak is really due to wave motion and does not reflect some 'input scale' of turbulent energy since even a buoyancy subrange region should not produce a slope greater than n^{-3}. (Lin et al 1969). A similar analysis of data obtained at 200 m in convective conditions yielded spectral slopes of approximately $n^{-5/3}$ extending down to frequencies of about 10^{-2} sec^{-1}, unstable phase angles and low coherence values (typically from 0.2 to 0.5).

5. <u>The structure of the wave</u>:- In order to study the development of the wave, a numerical band pass filter was applied to the data. This had a bandwidth which extended from .0016 to .0045 sec^{-1} and was formed by linearly combining three of Craddock's unitary filters (see Craddock, 1968). Figure 6 shows plots of the filtered data as a function of time. The most remarkable feature of these traces (see Fig. 6(b)) is the reversal in the sign of the W trace at 46 metres compared with those at 183 and 93 metres, (i.e. there is a "mirror-image" effect). Some insight into this phenomenon may be obtained by considering the two dimensional wave equation,

$$Z = A \sin (kx - \omega t) \qquad (2)$$

(where Z is the vertical displacement, A is the amplitude, k is the wave number, ω is the frequency in radians sec^{-1} and x and t are positions in the horizontal and time respectively). It follows that,

$$w = \frac{dz}{dt} = -(A\omega)\cos(kx - \omega t) \tag{3}$$

and

$$\frac{dz}{dx} = (Ak)\cos(kx - \omega t) \tag{4}$$

Now if α is the angle of inclination of the wave surface then $\tan\alpha = \frac{dz}{dx}$ and it follows that:-

$$w = c(z)\tan\alpha \tag{5}$$

where $c(z)$ is the velocity of the wave relative to the air at height z $(= \frac{\omega}{k})$. The observed period of the wave τ_o, if the wave is travelling in the same direction as the mean wind, is given by

$$\tau_o = \frac{\lambda}{V(z) + c(z)} \tag{6}$$

(where λ is the wavelength of the wave and $V(z)$ is the wind speed at height z) and it can be seen from Fig. 5 that this remains nearly constant. Thus if it is accepted that λ is a very weak function of z, then it follows that:-

$$V(z) + c(z) \approx \text{const.} \tag{7}$$

Over the height interval 183 to 46 metres, $V(z)$ increases by 2 metres so it follows from (7) that $c(z)$ must have decreased over the same height change. In fact it follows from the 'mirror-image' effect and equation (5) that it must actually have changed sign over this interval or in other words the wind was blowing over the wave in the opposite direction at 46 metres to that at 183 or 93 metres. These deductions and the observed values of $V(z)$ impose the following limits on the phase velocity at 183 metres:-

$$0.6 < c(183) < 2 \text{ m s}^{-1} \tag{8}$$

It is also possible to derive the value of $c(183)$ from the filtered w-trace at this height since from equation (3) the amplitude of the oscillations of the vertical velocity, is given by:-

$$A_w = A\omega = 2\pi A n \tag{9}$$

where n is the frequency of the wave. The required A_w's may be obtained by using the points on the filtered T-trace where T=0 to define the turning points on the corresponding w-trace. This minimises any advective effects and overcomes the complications introduced by the variation of $c(z)$ (see below). The A's may be read from the wave amplitude trace which is reproduced in Fig. 7 (this was produced from the filtered T-trace and the observed temperature gradient - it includes an adjustment to compensate for advection). This gives an overall average of .0006 $\sec^{-1}$ for n. Equation (6) may be recast (using $c = \lambda n$) as,

$$\lambda = \frac{V(z)}{n_0 - n} \tag{10}$$

and the value of n_0 may be derived from the spacing of the crests and troughs in Fig. 7. If this value of .0033 $\sec^{-1}$ and $V(183)$ = 3.6 metres/second are substituted into equation (10) it follows that $\lambda \sim 1.3$ km and hence that:-

$$c(183) = \lambda n \approx 0.8 \, m s^{-1}$$

which is within the range of values required to explain the reversal in the W-trace between 93 and 46 metres.

If $c(183) = 0.8$ ms^{-1}, $V(183) = 3.6$ ms^{-1} and $V(8) = 0.4$ ms^{-1} then it follows from equation (7) that $c(8) = 4.0$ ms^{-1}. Now it can be shown (see Gossard et al (1970)) that,

$$c(z) = \frac{\Delta p(z)}{\rho \, \Delta V(z)} \tag{11}$$

(where ρ is the density of the air $\approx 1.3 \times 10^{-3}$ gm/cc, ΔV and Δp are the amplitudes of the wind speed and pressure fluctuations at height z). If this equation is applied to the observations at 8 m with $\Delta V = 1$ ms^{-1} then

$$\Delta p(8) = 0.5 \, mb$$

This value is not incompatible with the record of the aneroid barometer during this period.

The change in sign of c from a positive value at 183 m to a negative one at 43 m implies that the intrinsic frequency (n) of the wave also became negative. This may indicate that the phenomenon of critical layer absorption occurred (see Bretherton, 1969). Briefly, the theory indicates that a wave packet moving in the vertical in a shear flow retains a constant horizontal wave number and frequency relative to the ground. This latter point was confirmed in this observation. However the theory also indicates that the wave should not penetrate the critical layer. This appears to be at variance with the observations discussed above.

The variation in $C(Z)$ helps to explain why $\Phi_{WT}(n)$ is not about 90°. With a constant phase velocity the extremes in the W trace would be associated with zeros in the T trace. In this study $C(Z)$ decreased with height so maxima in the W-trace should lag the zeros in the T trace. However $\Phi_{WT}(n)$ will also depend on temperature advection and the detailed wave shape. It has already been shown that the amplitude varied with time and that there was a time lag between the traces at 183 m and 93 m. Thus in general $\Phi_{WT}(n)$ may not have the expected value and could vary with time. The spectral analysis will of course yield an average value of $\Phi_{WT}(n)$.

The variations in the u-component caused by the wave will be affected by the proximity of the ground. Thus when the amplitude of the wave is compatible with the height above the surface, there will be a significant compression/ rarefaction of the streamlines:-

$$V_c(z) = \frac{V(z-A)}{1 + A/z} \quad \text{- at a crest}$$

$$V_T(z) = \frac{V(z+A)}{1 - A/z} \quad \text{- at a trough} \qquad (12)$$

(where $V(z \pm A)$ are the undisturbed wind velocities at $z \pm A$). The combination of this effect with the variation of V with height means that the phase angles between u and the other two variables (ie W and T) could be quite different from the expected values (see Section 4). An idea of the importance of these effects in the present study may be obtained from the amplitude versus time trace in Fig. 7. If the typical crest/trough amplitude is taken as about 50 metres at 183 metres and if $V(z)$ = 3.6 metres/sec at all levels, then it follows that $V_C(183)$ = 2.8 metres/sec and $V_T(183)$ = 5.0 metres/sec. Thus even in the absence of vertical wind shear this effect would have introduced an asymmetric variation of 2.2 metres/sec on the wind trace at 183 metres.

6. <u>The occurrence of turbulence</u>:- As has been pointed out earlier (ie Sections 3 and 4) turbulent activity was insignificant at 183 metres but generally increased with decreasing z (see Table 1). At 46 and 93 metres the turbulence appeared in the form of bursts lasting about 4 or 5 minutes and even at 8 metres where the turbulence was almost continuous, there were periods of increased activity (see Fig. 1). These "bursts" are clearly associated with the amplitude structure of the wave and it is interesting to note that the bursts at 46 metres precede those at 93 metres. This probably reflects the fact that at these levels the wind was blowing over the wave in opposite directions - the main "breakdown" region being expected on the downwind side of the crests (eg Rayment and Readings (1974)).

It appears from these results that the perturbations introduced by the wave were sufficient to cause turbulence at 46 metres and 93 metres but not at 183 metres. Prior to the arrival of the wave the Richardson numbers were:-

Height (metres)	Richardson Numbers
183	6
93	4
46	2

so it is not surprising that the flow at the 183 metre level, as opposed to that at 93 or 46 metres, remained laminar during the passage of the wave.

The reduction of stability during the passage of a gravity wave has been considered in some detail by Gossard et al (1973) but their results are not directly applicable to the present observations. However there is no real doubt that the reduction of the Richardson numbers at the crests of the wave was caused by the enhancement of wind shear accompanying the tilting of the isentropic surfaces. This phenomenon has been considered by Scorer (1969) and it follows from his analysis that:-

$$Ri_{new} = \left[\frac{1}{Ri_{old}} + \frac{N^2 A^2}{c^2(z)} + \frac{2AN}{c(z)\sqrt{Ri_{old}}} \right]^{-1} \qquad (13)$$

provided the compression of the θ-surfaces is neglected. All the quantities on the right-handside of this equation are known for the 183-metre level so it is possible to check whether the lack of turbulence at this level is reasonable or not. Thus taking N = .0167, A =50 metres and $C(183)$ = 0.8 metres/sec, gives $Ri_{new} \sim 0.5$ and this value is quite compatible with laminar flow (eg Woods (1969)). This analysis cannot be repeated at the other levels because A is not known.

Concluding remarks:- This paper has presented the results of a detailed study of a gravity wave in the first 200 m. of the Earth's boundary layer. It has been shown that although many of its features can be understood in terms of simple wave theory, many other factors complicated the situation. These included advection, vertical wind shear, turbulence and the proximity to the surface. Thus the interpretation of waves in such conditions becomes very complicated. Simplification of the data by numerical filtering and spectral analysis would appear to be a useful first step. Close to the surface the values of the phase angles cannot be used to distinguish between waves and turbulence, but the self-consistency requirement should still help to indicate the presence of waves. This fact together with high coherences and peaks in the spectra, seem to form the most promising diagnostic approach. However in the presence of significant turbulence it is difficult to see how even these techniques will help unless the wave and turbulence fall in different frequency bands.

One of the most interesting aspects of this study was the occurrence of wave induced turbulence at the middle levels and possibly the enhancement of turbulence at the lowest level. The simple analysis presented showed that this was not an unexpected result. However the importance of the phenomenon from the general viewpoint of turbulence in stable conditions obviously merits further study with more extensive instrumentation.

TABLE 1

Probe Height (metres)	σ_w (cms sec^{-1})*
183	1
93	8
46	21
8	24

*based on frequency interval from 10^{-2} to 10^{-1} sec^{-1}.

TABLE 2

Source of data	Component	Phase Angle	Coherence
Present study - (183 m)	$\overline{wT}$	48°	0.98
" " "	$\overline{uT}$	72°	0.96
" " "	$\overline{uw}$	22°	0.98
Axford (1971)	$\overline{wT}$	78°	0.90
"	$\overline{uT}$	160°	0.90
"	$\overline{uw}$	98°	0.85

List of Figure Captions:-

Figure 1:- Traces of the basic quantities T, ϕ and V (for each of the four probes) versus time. The letter I on the ϕ trace at 8 m signifies interference at this time.

Figure 2:- (A) to (D) give the plots of the 30 sec average values of T, u and W for the four probes.

Figure 3:- The wind direction trace at 16 m. Inset are the wind direction/speed traces at 46 m recorded by the anemograph.

Figure 4:- Plots of the dry bulb temperature (▲), dew point temperature (X) and virtual potential temperature (O) versus height from the 2300/0200 GMT Balthum ascent.

Figure 5:- (A). Plots of the power spectra from the probe at 183 m with the following symbols

	Symbol	Units
$n\,S_W\,(n)$	●	$m^2\,s^{-2}$
$n\,S_U\,(n)$	▲	$m^2\,s^{-2}$
$n\,S_T\,(n)$	□	$^oC^2$

(B) Plots of the

(i) cross spectral amplitudes

(ii) phase angles

(iii) coherences

for the covariances $\overline{wT}, \overline{uT}, \overline{uw}$ from the probe at 183 m.

Figure 6:- Plots of the filtered u, w and T data from the four probes versus time.

Figure 7:- The wave amplitude at 183 m versus time, (derived from the filtered T trace and the observed temperature profile, taking account of the variation of the temperature profile with time).

List of References

Axford, D. N. (1971) "Spectral analysis of an aircraft observation of gravity waves". Quarterly Journal of Royal Meteorological Society, 97, (313-321).

Busch, N. E. (1969) "Waves and turbulence". Radio Science 4, (1377-1379).

Bretherton, F. P. (1969) "Waves and turbulence in stably stratified fluids", Radio Science, Vol. 4, Number 12, pp. 1279-1287.

Craddock, J. M. (1968) "Statistics in the Computer Age". English Universities Press, pp. 214.

Gossard, E. E., Richter, J. H. and Atlas, D. (1970) "Internal waves in the atmosphere from high resolution radar measurements". Journal of Geophysical research, 75, (903-913).

Gossard, E. E., Jensen, D. R. and Richter, J. H. (1971) "An analytic study of tropospheric structures as seen by high resolution radar". Journal of Atmospheric Sciences, 28, 794-807.

Gossard, E. E., Richter, J. H. and Jensen, D. R. (1973) "Effects of wind shear on atmospheric wave instabilities revealed by FM|CW radar observations". Boundary-Layer Meteorology, 4, (113-131).

Lin, J. T., Panchev, S. and Cermak, J. E. (1969) "A modified hypothesis on turbulence spectra in the buoyancy subrange of stably stratified shear flow". Radio Science, Vol. 4, No. 12, pp. 1333-1337.

Painter, H. E. (1970) "The tethered radiosonde". Meteorological Magazine, 99, (93-98).

Rayment, R. and Readings, C. J. (1974). "A case study of the structure and energetics of an inversion". Quarterly Journal of the Royal Meteorological Society, 100, (221 - 233)

Rayment, R. (1970) "Introduction to the fast fourier transform (FFT) in the production of spectra". Meteorological Magazine, 99, (261-270).

Readings, C. J. and Butler, H. E. (1972) "The measurement of atmospheric turbulence from a captive balloon". Meteorological Magazine, 101, (286-298).

Roach, W. T., Adams, R. J., Garland, J. A. and Goldsmith, P. (1973) "A field study of radiation fog". Faraday Symposia of the Chemical Society No. 7, (209-221).

Scorer, R. S. (1969) "The origins and forms of dynamic instability in clear air at high altitude". Proceedings AGARD NATO Special Meeting on Aerodynamics of Atmospheric Shear Flows, Advisory Group on Aeronautical and Research Development (Munich).

Stewart, R. W. (1969) "Turbulence and waves in a stratified atmosphere". Radio Science, 4, (1269-1278).

Woods, J. D. (1969) "On Richardson's number as a criteria for laminar-turbulent - laminar transition in the ocean and atmosphere". Ibid, (1289-1298).

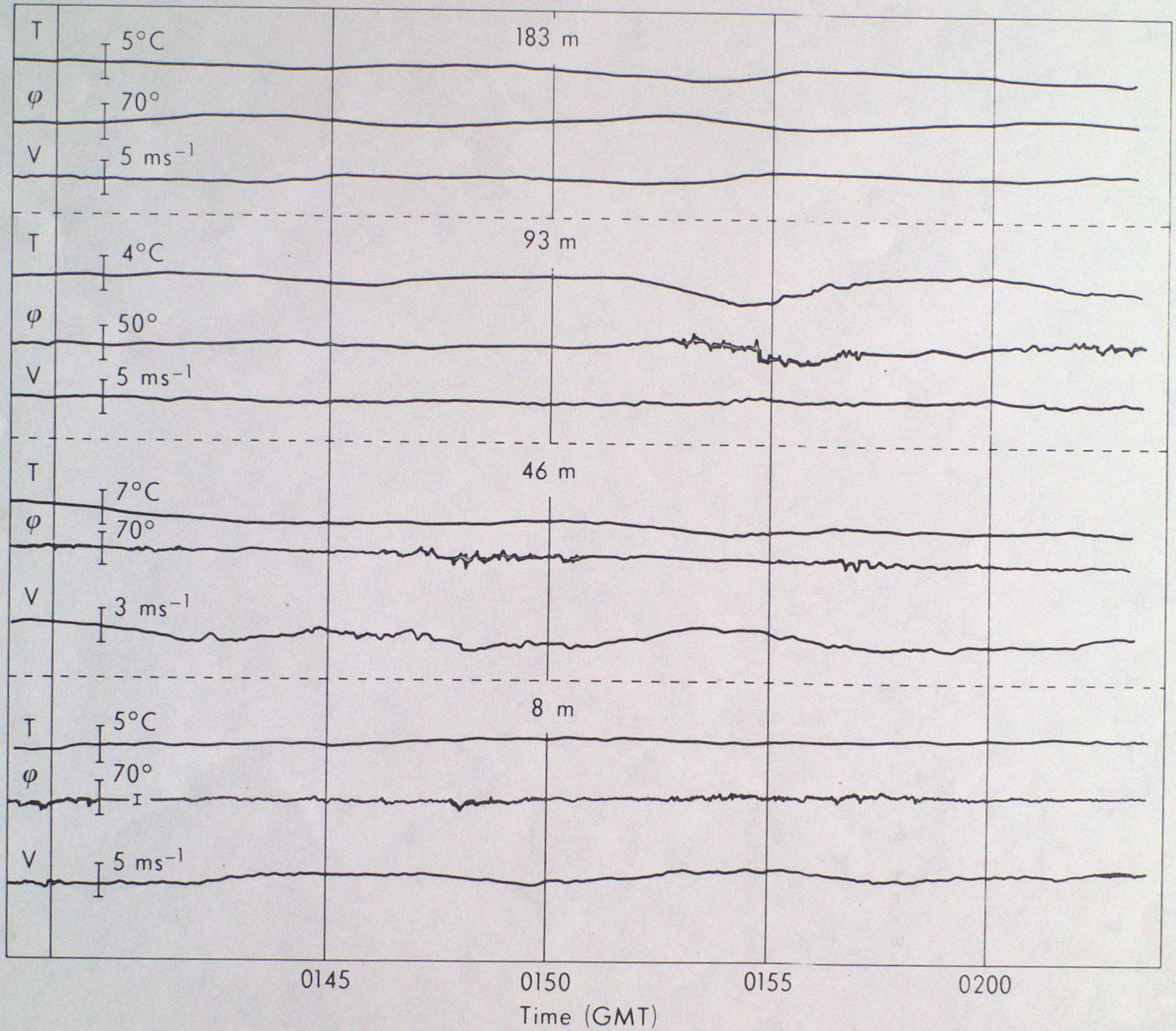
T
5°C
183 m
φ
70°
V
5 ms⁻¹
T
4°C
93 m
φ
50°
V
5 ms⁻¹
T
7°C
46 m
φ
70°
V
3 ms⁻¹
T
5°C
8 m
φ
70°
V
5 ms⁻¹
0145
0150
0155
0200
Time (GMT)

Figure 1

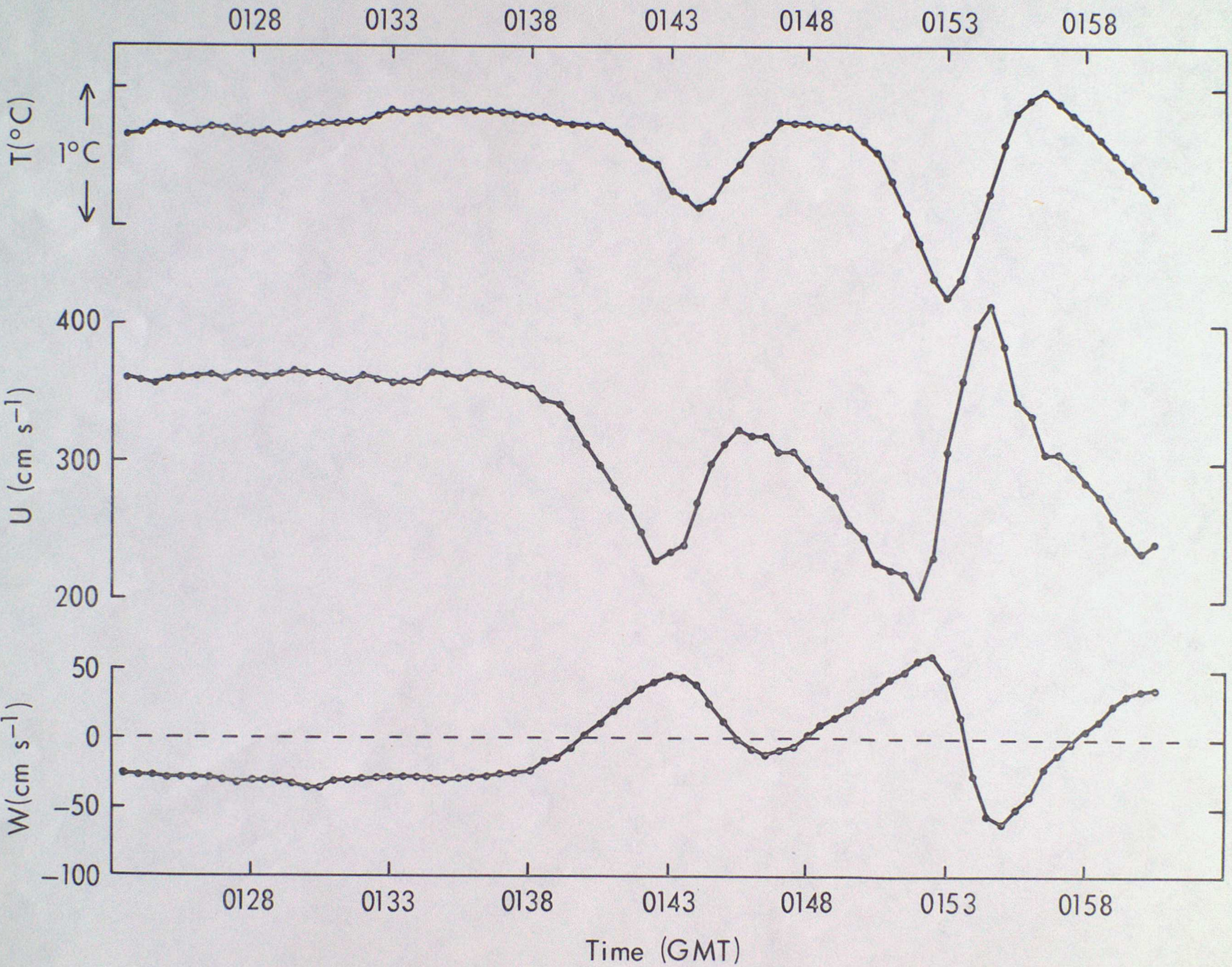

Figure 2a — 183 metres

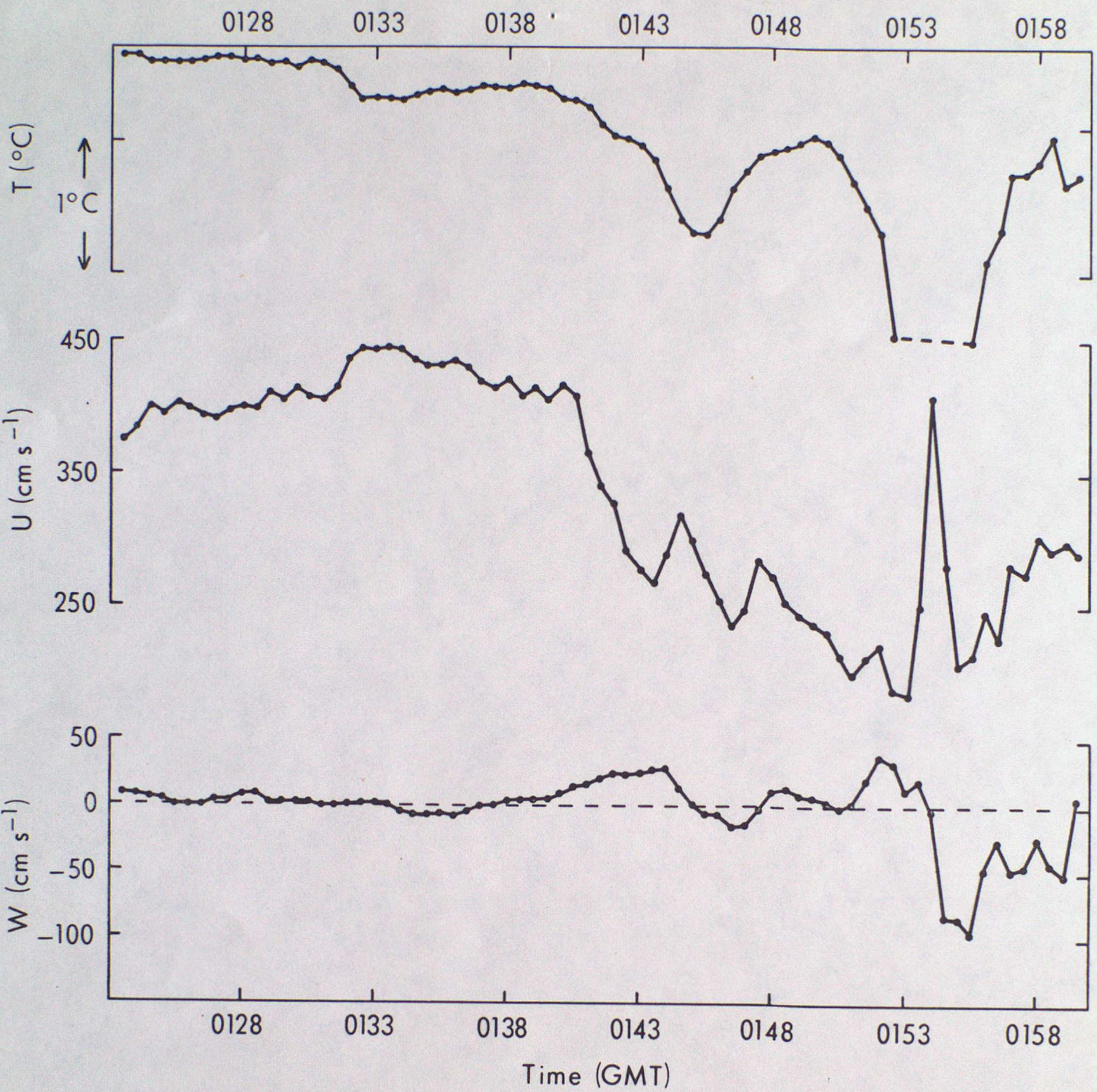

Figure 2b — 93 metres

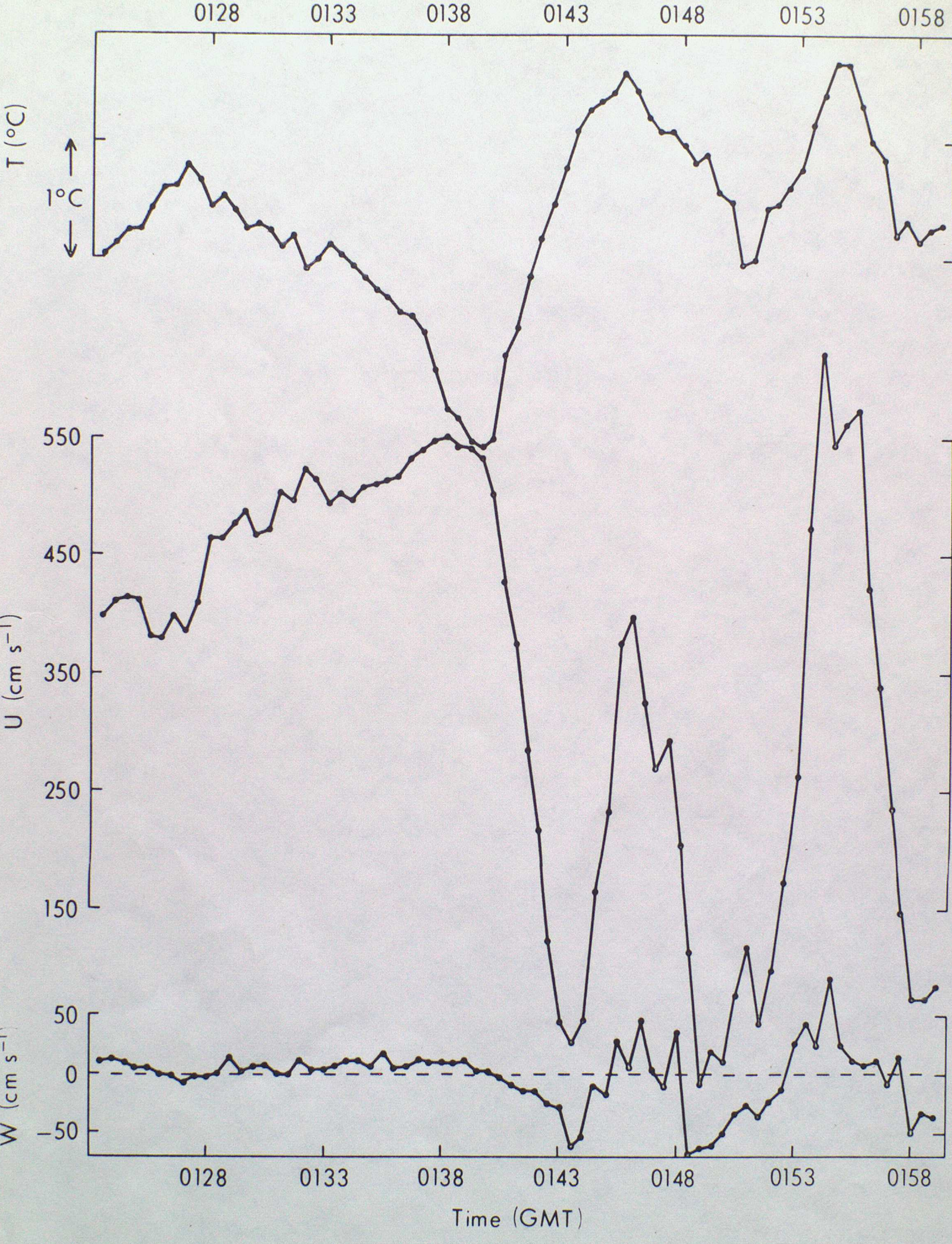

Figure 2c — 46 metres

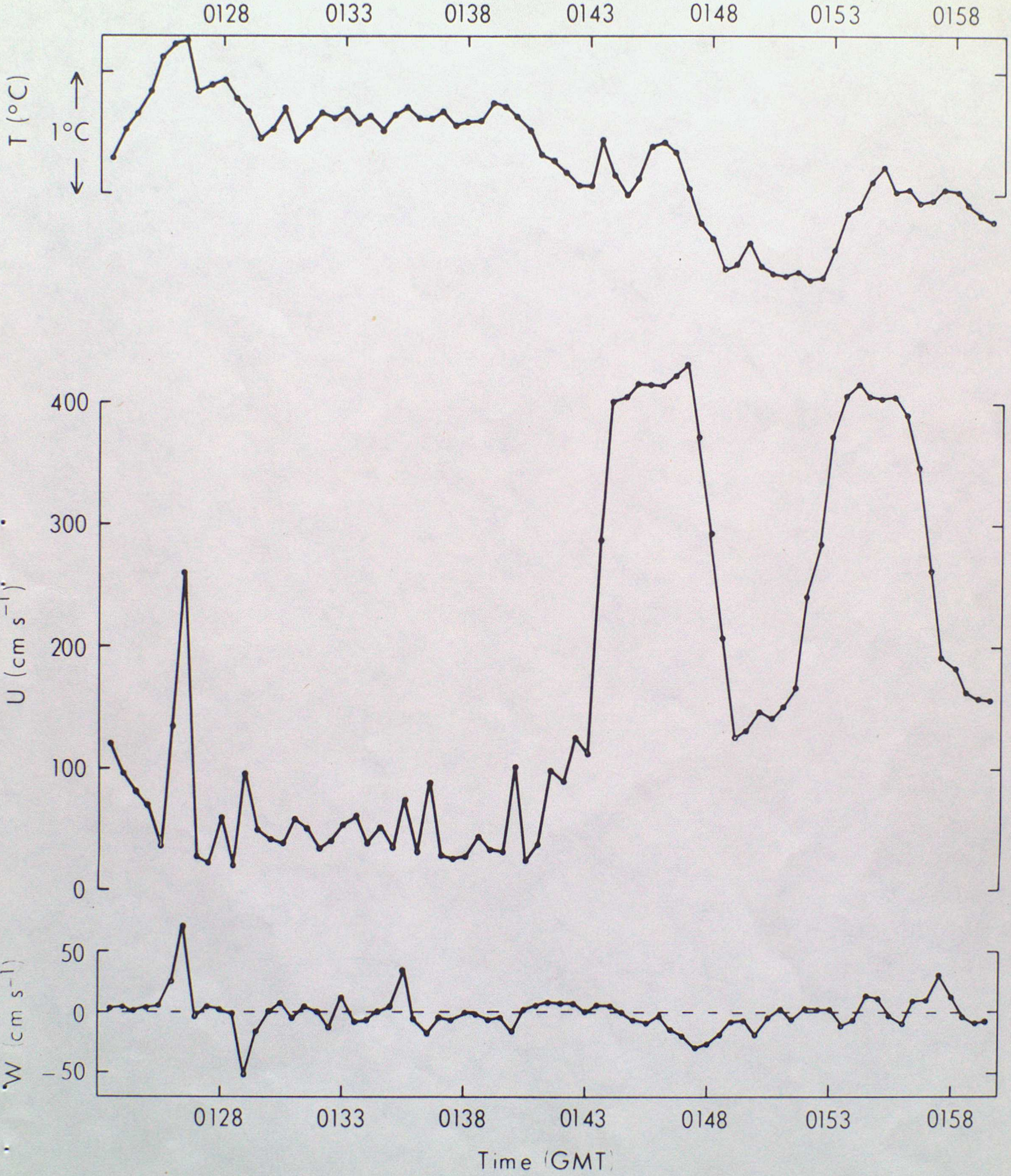

Figure 2d — 8 metres

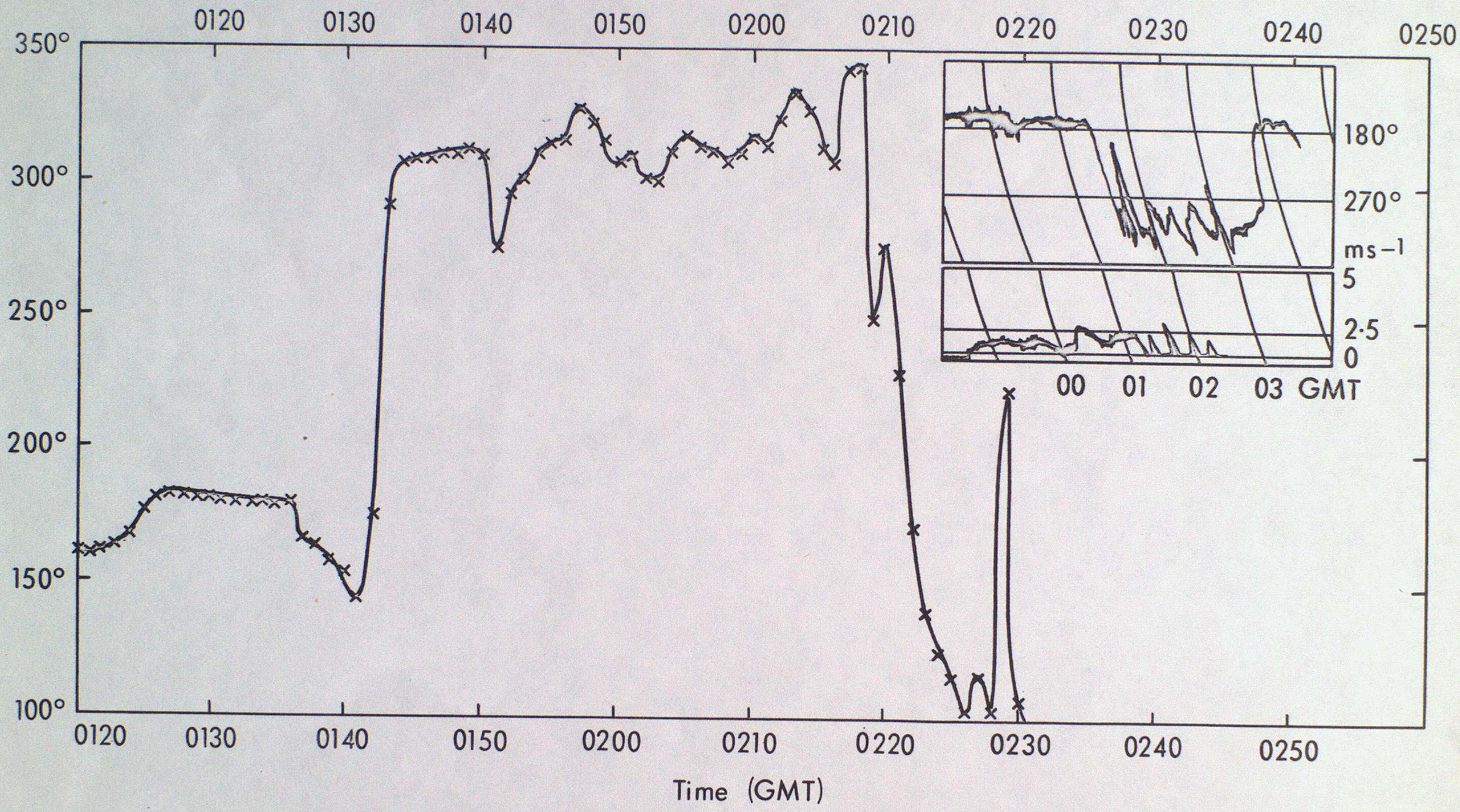
0120
0130
0140
0150
0200
0210
0220
0230
0240
0250
350°
300°
250°
200°
150°
100°
180°
270°
ms−1
5
2·5
0
00
01
02
03 GMT
Time (GMT)

Figure 3

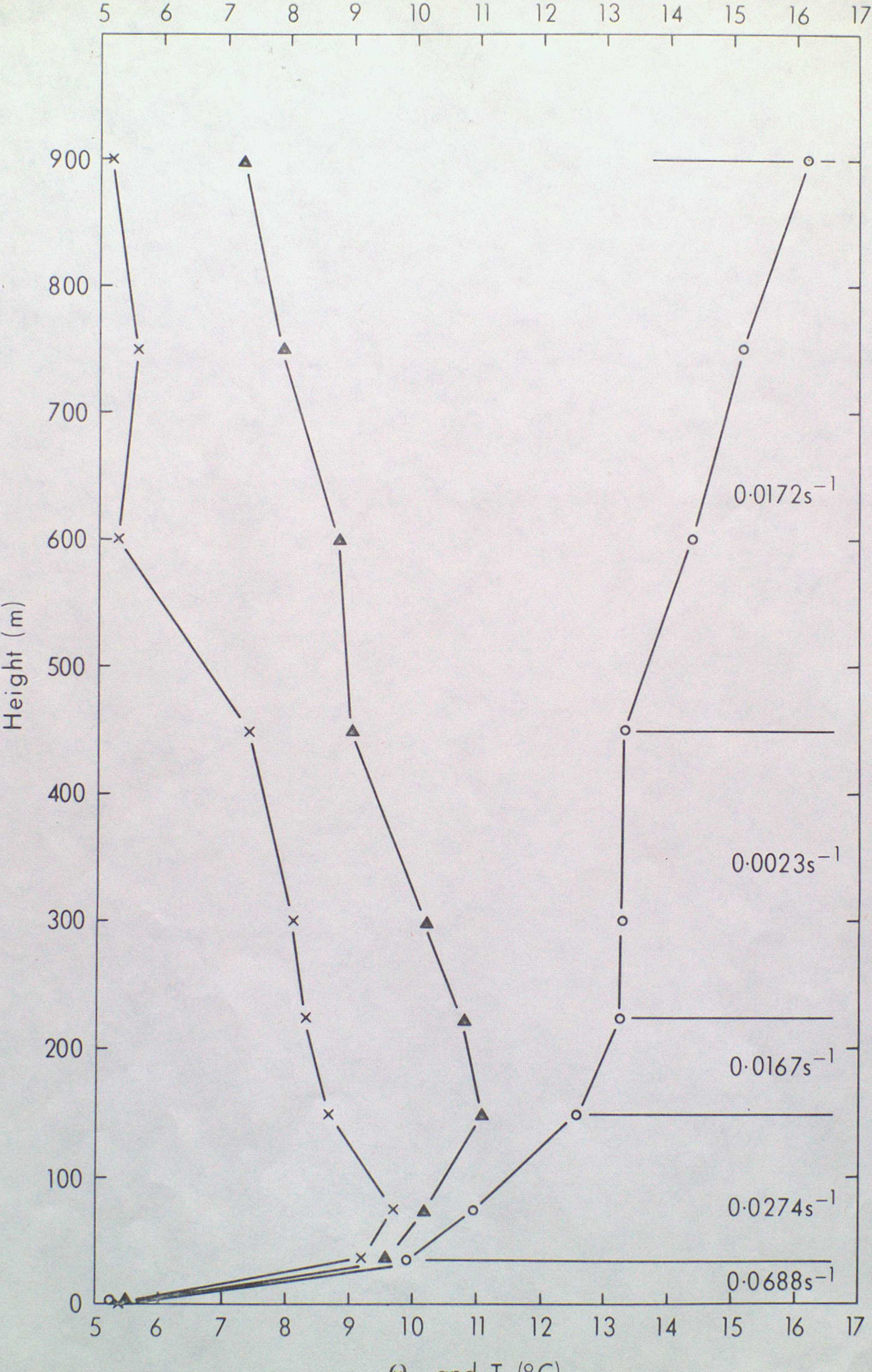

5 6 7 8 9 10 11 12 13 14 15 16 17
900
800
700
600
500
400
300
200
100
0
Height (m)
0·0172s^{-1}
0·0023s^{-1}
0·0167s^{-1}
0·0274s^{-1}
0·0688s^{-1}
5 6 7 8 9 10 11 12 13 14 15 16 17
Θ_v and T (°C)

Figure 4

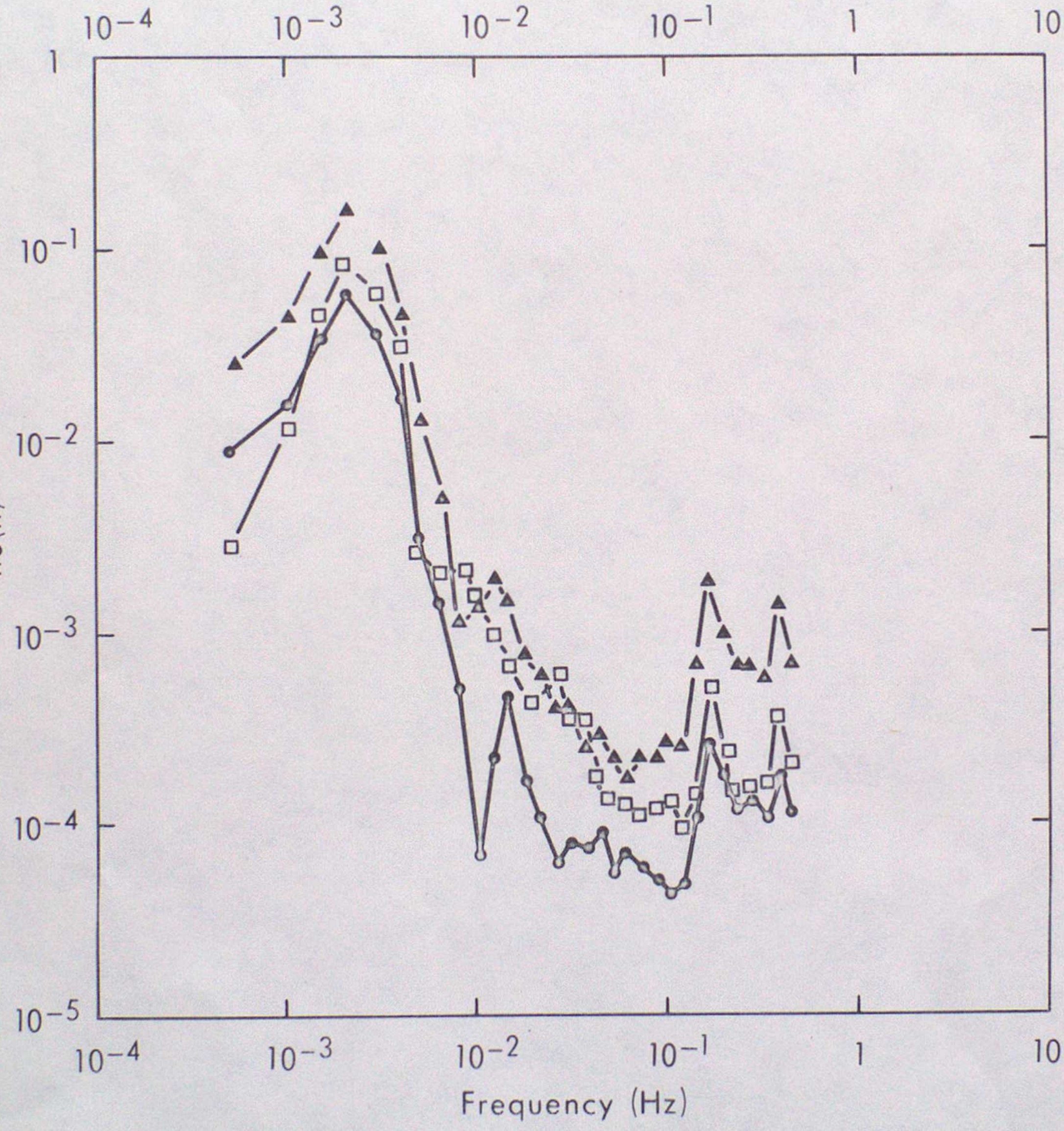

10^-4
10^-3
10^-2
10^-1
1
10
1
10^-1
10^-2
10^-3
10^-4
10^-5
nS(n)
10^-4
10^-3
10^-2
10^-1
1
10
Frequency (Hz)

Figure 5a

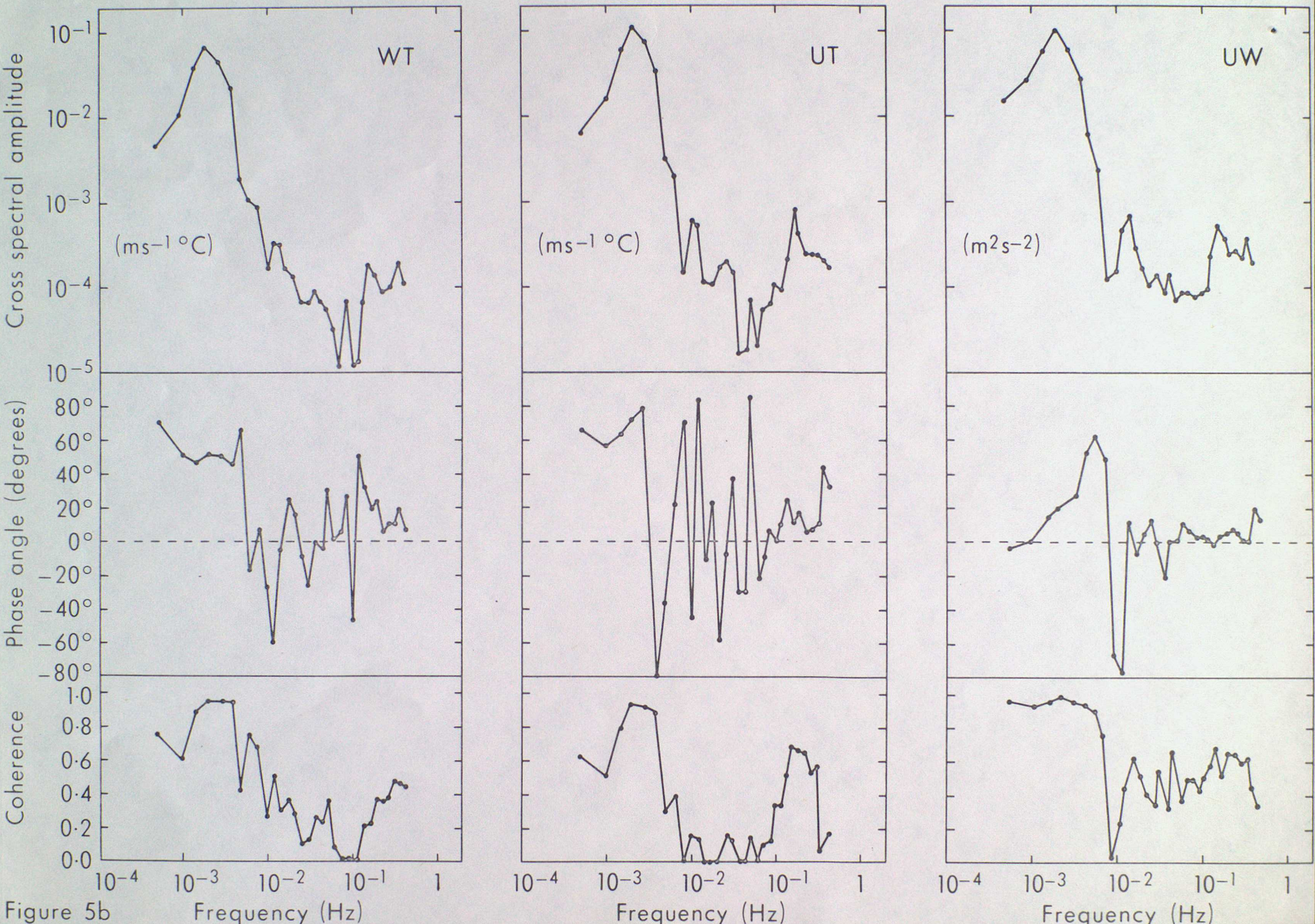

Cross spectral amplitude
Phase angle (degrees)
Coherence
WT
UT
UW
(ms-1 °C)
(ms-1 °C)
(m2s-2)
10-1
10-2
10-3
10-4
10-5
80°
60°
40°
20°
0°
-20°
-40°
-60°
-80°
1·0
0·8
0·6
0·4
0·2
0·0
10-4
10-3
10-2
10-1
1
Frequency (Hz)
Frequency (Hz)
Frequency (Hz)

Figure 5b

U Data

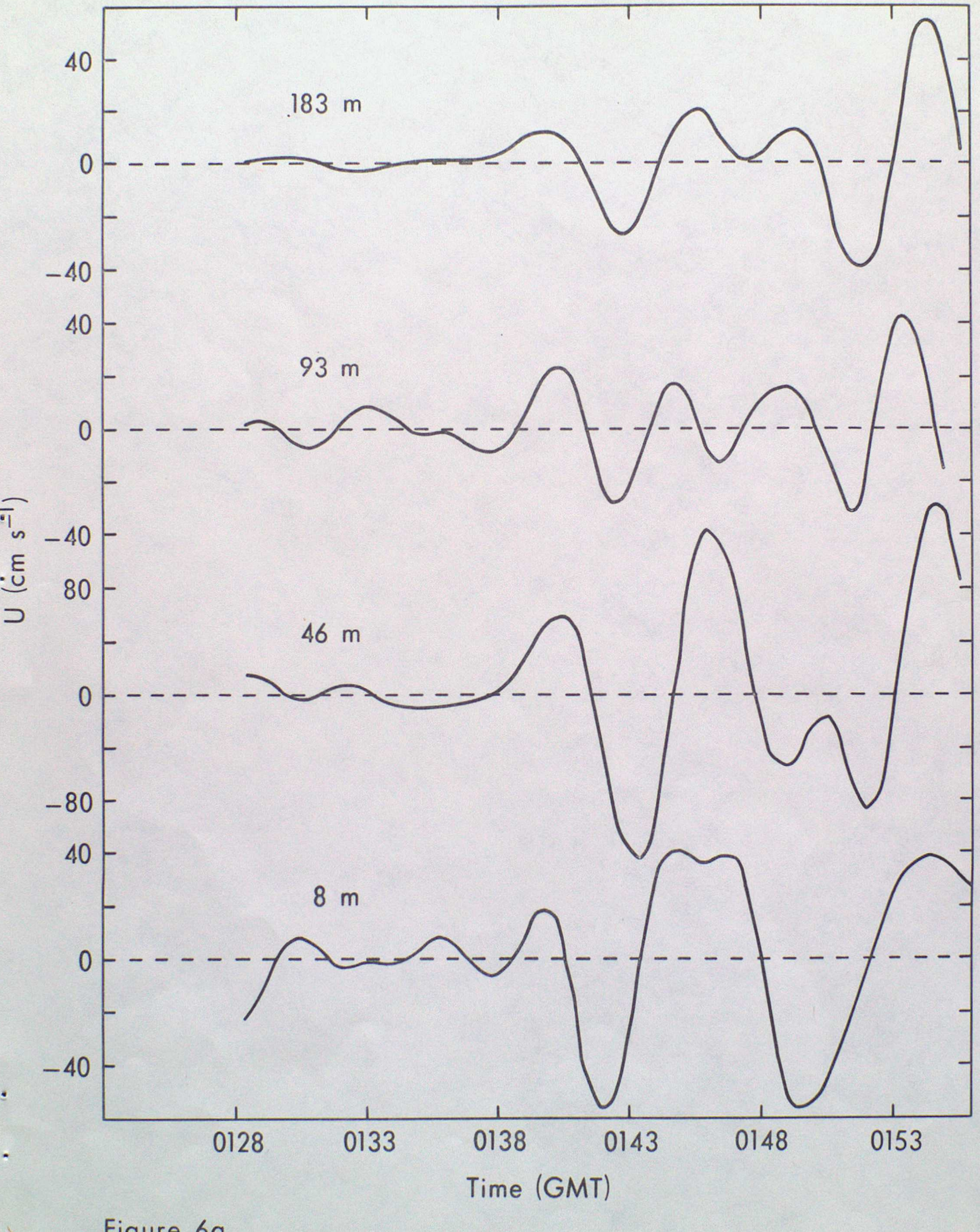

Figure 6a

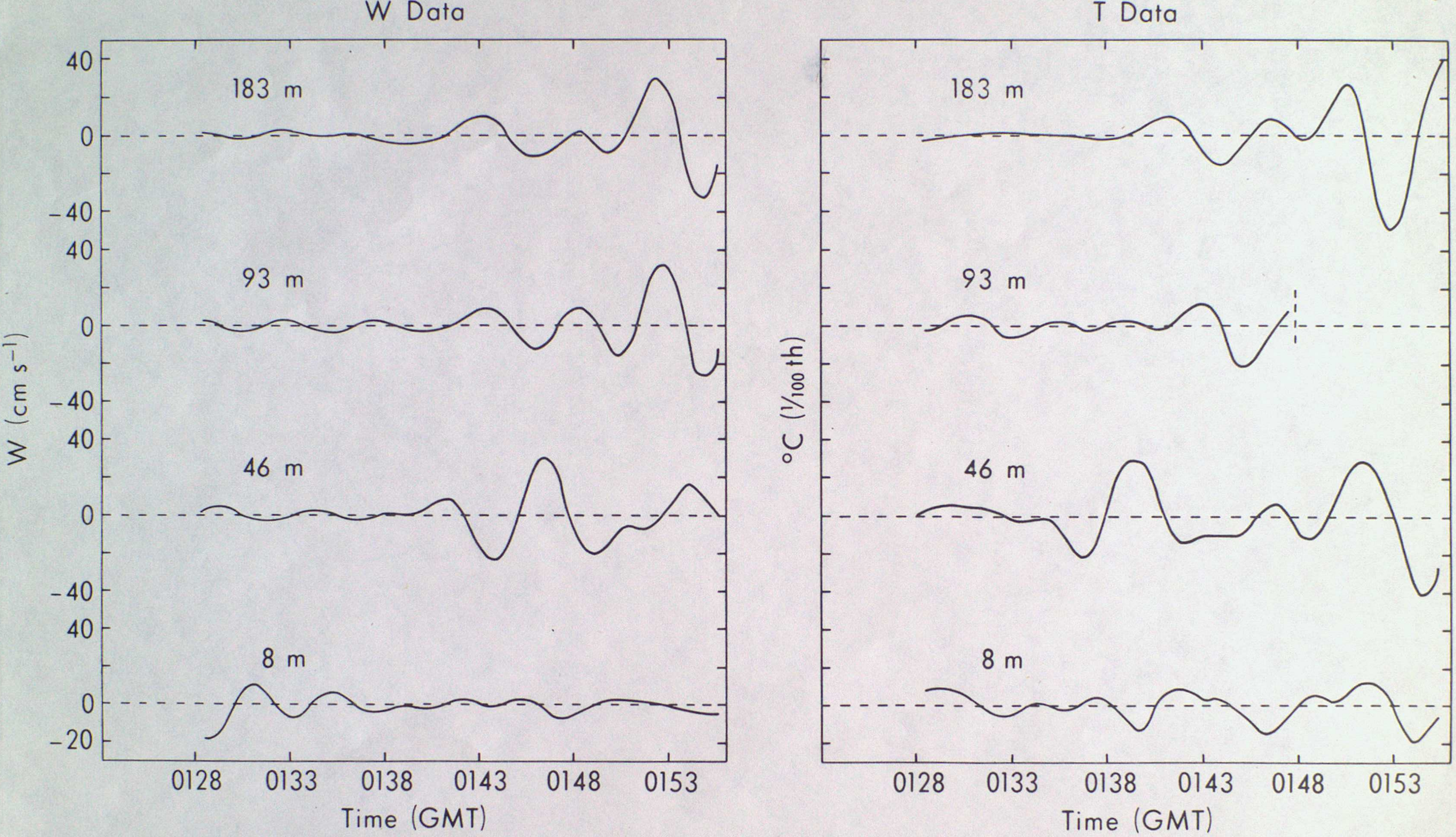
W Data
183 m
93 m
46 m
8 m
40
0
-40
-20
W (cm s^-1)
0128
0133
0138
0143
0148
0153
Time (GMT)
T Data
°C (1/100 th)

Figure 6b

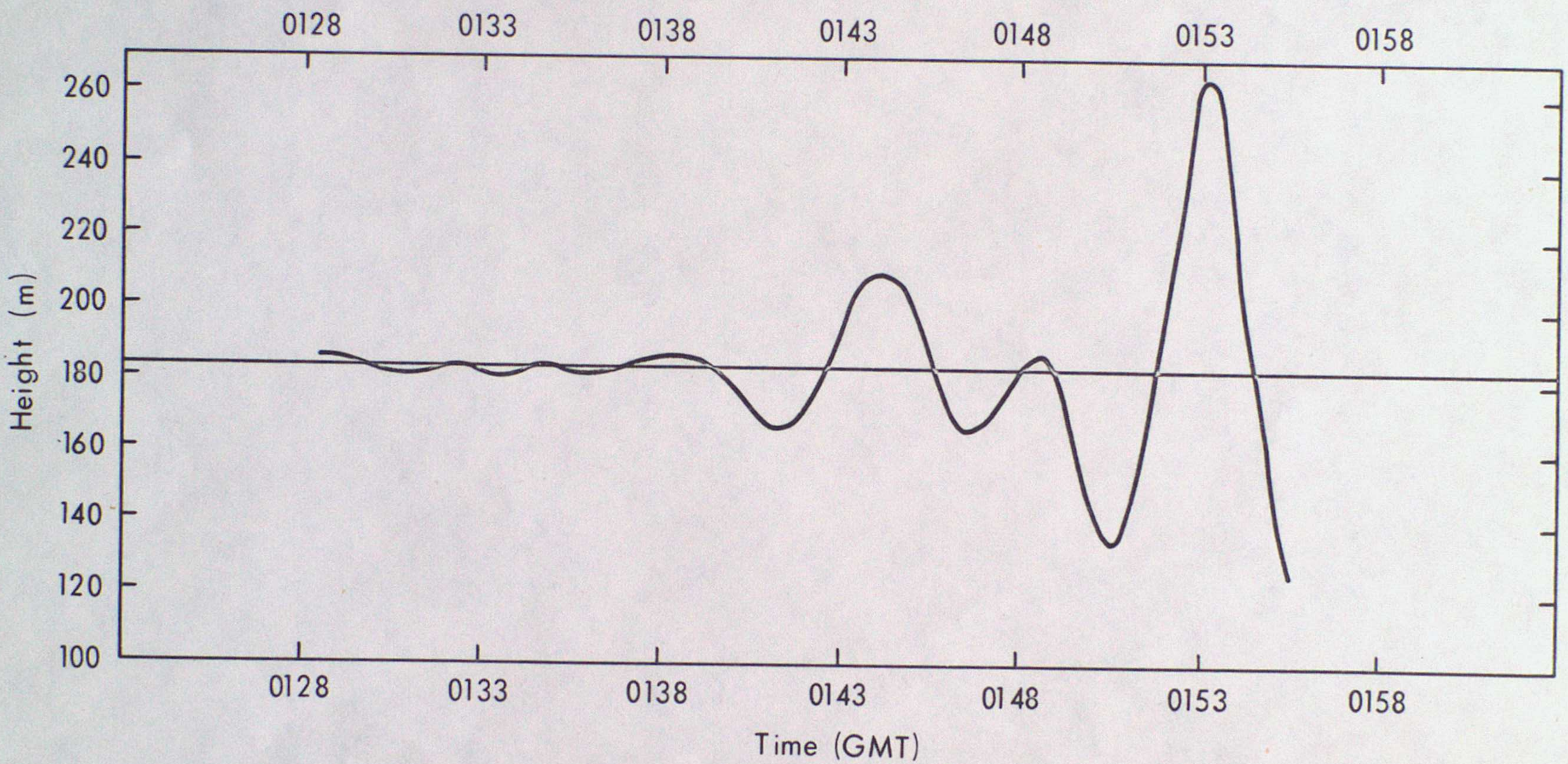
0128
0133
0138
0143
0148
0153
0158
260
240
220
200
180
160
140
120
100
Height (m)
Time (GMT)

Figure 7